Physica A 597 (2022) 127324

Contents lists available at ScienceDirect

Physica A

journal homepage: www.elsevier.com/locate/physa

Stochastic pursuit-evasion curves for foraging dynamics

Kellan Toman, Nikolaos K. Voulgarakis [*]

Department of Mathematics and Statistics, Washington State University, Pullman, 99164, United States of America

ARTICLE INFO

Article history:
Received 25 May 2021
Received in revised form 7 March 2022
Available online 31 March 2022

Keywords:
Animal foraging
Pursuit-evasion games
Persistent random walks
Tempered power-law distributions
Transient superdiffusion
Directional persistence

ABSTRACT

Many predator species attempt to locate prey by following seemingly random paths. Although the underlying physical mechanism of the search remains largely unknown, such search paths are usually modeled by some type of random walk. Here, we introduce the stochastic pursuit-evasion equations that consider the bidirectional interaction between predators and prey. This assumption results in a modulated persistent random walk that is characterized by three interesting properties: power-law or tempered power-law distributed running times, superdiffusive or transient superdiffusive dynamics, and strong directional persistence. Furthermore, the proposed model exhibits a transition from Brownian to Lévy-like motion with intensifying predator–prey interaction. Interestingly, persistent random walks with pure-power law distributed running times emerge at the limit of highest predator–prey interaction. We hypothesize that the system ultimately self-organizes into a critical interaction to avoid extinction.

1. Introduction

Many physiological and pathological processes are directly linked to the ability of living organisms to move. For instance, animal migration is essential in searching for food or a mate [1]; however, this phenomenon is also responsible for the faster and wider spread of diseases [2]. Cell motility, as a different example, is vital for a healthy immune system response, but movement of cancerous cells also leads to metastasis [3]. Thus, understanding the movement of organisms will address fundamental questions in biology and help develop new therapeutic strategies and better policies for public health and safety.

Living organisms often follow a species-specific strategy in the presence of signals generated by a target of interest. They receive and process these signals and then execute their strategy to move towards the target. In the absence of external stimuli, many species attempt to locate a target by moving in a seemingly stochastic fashion. This movement may result from simple random and memoryless decisions or decisions based on learning, memory, or interaction with the environment. Therefore, mathematical modeling of such paths may require implementation of various Markovian, non-Markovian or even deterministic processes [4–10].

Although no general theory exists explaining the underlying physical mechanism of foraging, some predators have been observed undertaking long persistent walks that are interrupted by random short-term reorientations. Among others, Lévy walks (LWs) are a class of stochastic processes that have been used extensively to model such search patterns. LWs move persistently with finite speed for running times τ that are power-law distributed, i.e., $P(\tau) \sim \tau^{-\mu}$, where $1 < \mu < 3$ [11,12], and then change direction with turning angles that are uniformly distributed. Due to the finiteness of the speed, the same power law distribution characterizes persistent running distances, l, of LWs ($P(l) \sim l^{-\mu}$). However,

---

[*] Corresponding author.
E-mail address: n.voulgarakis@wsu.edu (N.K. Voulgarakis).

https://doi.org/10.1016/j.physa.2022.127324
0378-4371/

in a real experimental setup, where space and time is finite, the recorded walk may be described better by a tempered power-law distribution, which is a power law bounded by an exponential:

$$P(\tau) \sim \tau^{-\mu} e^{-\tau/\tau_c}. \tag{1}$$

Here, τ_c indicates the critical time the distribution starts deviating from pure power laws. For the remainder of this paper, we define Levy-like RWs as stochastic processes that possess power-law or tempered power-law step distributions.

Other stochastic processes, such as correlated RWs, composite RWs, or intermittent RWs have proven successful in modeling search patterns, and in many cases give very similar results to LWs. Correlated RWs, for instance, are stochastic processes mainly based on the Ornstein–Uhlenbeck (OU) equation and its extensions to include multiplicative noise and memory effects [13–18]. Such approaches result in correlated persistent RWs capturing some of the properties of foraging dynamics. Composite RW, as a different example, is a mixture of two or more simple RWs [19]. Intermittent RWs is another, recently introduced, stochastic process for foraging paths [20–22]; in this process, the predator randomly switches between Brownian search motion and ballistic relocation. Lévy-like RWs can also emerge from the chaotic behavior of a deterministic nonlinear system of equations [8,9,23].

Generally speaking, there are two main schools of thought in modeling foraging patterns. Evolutionists believe that organisms must have evolved through natural selection to adopt LWs movement simply because power-law distributed displacements optimize search efficiencies [24–32]. Emergentists, on the other hand, believe that LWs may simply result from the interaction of predators with the environment, without necessarily optimizing their searching efficiency [33–41]. In this study, we embrace both hypotheses but from a different perspective. Predators utilize the search patterns that either spontaneously emerge due to interaction with the environment or are adapted through natural selection to enhance encounters with prey. We primarily hypothesize that prey are subject to the same assumptions. Specifically, prey also utilize natural selection and interaction with the environment to develop random avoidance paths that reduce encounters with predators. Thus, foraging is, at a bare minimum, a pursuit-evasion process between the predators and prey. Any improvement in the predator's searching skills is subsequently accompanied by an improvement in the prey's avoidance skills and vice versa.

The pursuit-evasion stochastic process presented in this work is based on simple stochastic differential equations that are straightforwardly applicable in all three dimensions. A few notable characteristics of this approach are tempered power law distributed running times, transient superdiffusion behavior, and strong directional persistence. Interestingly, our model undergoes a transition from Brownian to Levy-like RWs with an increasing predator–prey interaction. We hypothesize that both predators and prey eventually self-organize to a critical state that minimizes the chances of extinction of the whole ecosystem [29,42].

This paper is organized as follows. Section 2.1 presents the traditional pursuit equation; 2.2 introduces our stochastic pursuit-evasion model. Section 3 details numerical and analytical results. Specifically, Sections 3.1.1, 3.1.2, and 3.1.3 present the distribution of running times, the superdiffusive behavior, and the directional persistence, respectively, of the proposed model in one dimension (1D). Section 3.2 briefly presents the same results in two dimensions (2D) and three dimensions (3D). Comparison with similar existing mathematical models is also discussed. We conclude this paper by summarizing our work in Section 4.

2. The model

2.1. Pursuit model

The traditional pursuit equation describes the trajectory of a predator chasing an unsuspecting prey moving on a predefined deterministic trajectory [43,44]. It is important to underline that the prey has already been located and being chased by a predator in close proximity. Thus, this type of pursuit is not to be confused with foraging, where the predator tries to first find a prey. A traditional example usually used in textbooks to illustrate this toy-model is the dog-cat pursuit on a 2D plane [43,44]. The cat is assumed to follow a deterministic path, $\boldsymbol{R}_t$, where t represents time. The dog's strategy is rather simple as it moves directly towards the cat with speed v_r. With these simple assumptions, the position of the dog, $\boldsymbol{r}_t$, is given by the following equation:

$$\frac{d\boldsymbol{r}_t}{dt} = v_r \frac{\boldsymbol{R}_t - \boldsymbol{r}_t}{\|\boldsymbol{R}_t - \boldsymbol{r}_t\|}, \tag{2}$$

where $\|\cdot\|$ is the Euclidian norm. This equation was first introduced by Pierre Bouguer in 1732 [45], but the term *pursuit curves* was coined in 1859 by George Boole in his book, *Treatise on Differential Equations* [46]. In general, the speed of the dog can be proportional to that of the cat: $v_r \sim |\dot{\boldsymbol{R}}_t|$. In what follows, we assume for simplicity that the length and time are both dimensionless. The differential equations are all solved numerically using the Euler or Euler–Maruyama method [47].

Fig. 1a illustrates a representative curve of this problem. The dog moves directly towards its target at any point in time and eventually catches the cat if $v_r > v_R$. Similar direct pursuit curves can be found across taxa, even at a scale that is smaller by five orders of magnitude, such as the pursuit of a bacterium by a white blood cell as shown in Fig. 1b. This trajectory was derived from the iconic 16 mm movie made by David Rogers at Vanderbilt University, Nashville, USA

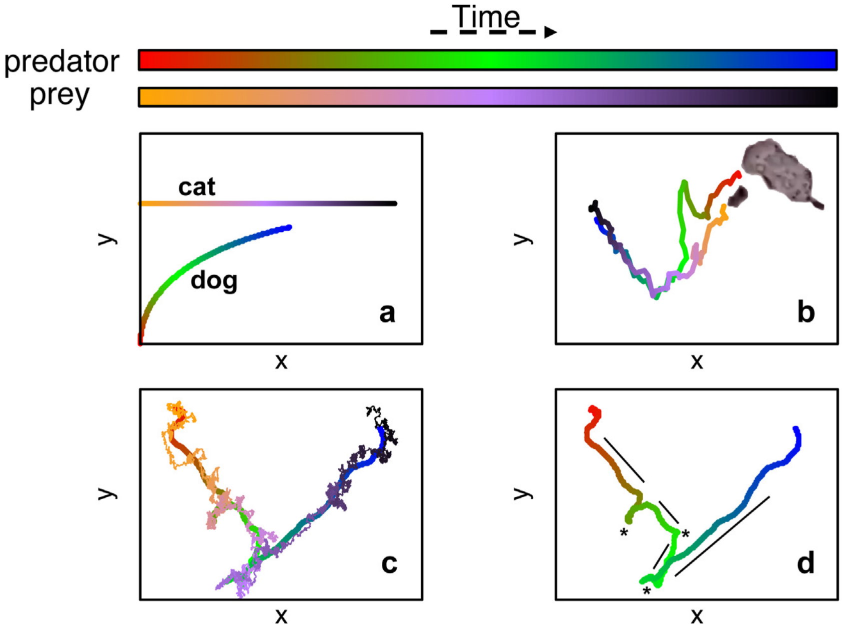

Fig. 1. Examples of predator–prey pursuit curves. Time increases according to the palettes shown on the top of the Figure. (a) Deterministic dog-cat pursuit curve. The dog always points directly to the cat's location. (b) *Neutrophil* (large object) hunting a *Staphylococcus aureus* bacterium (small object) [48]. (c) Stochastic pursuit curves of a predator chasing a Brownian particle. Here, $D_R = 1$ and $v_r = 6$. (d) Same as in (c), but only the trajectory of the predator is shown for clarity. Straight lines and stars indicate the runs and tumbles, respectively.

in the 1950s [48]. This movie gives the impression that, similarly to the dog-cat pursuit, the white blood cell directly chases a bacterium. A striking difference as compared to the deterministic example is the stochastic nature of the pursuit curve. This stochasticity is rather expected at such small scales where thermal fluctuations dominate the trajectories of molecules and nano-to-micro-scale structures.

Despite the randomness of the curves, Eq. (2) can still describe this problem if one assumes that the bacterium is moving along a predefined stochastic path. The result of such a stochastic pursuit equation is shown in Fig. 1c, where the pursuer is chasing a Brownian particle, i.e., $\boldsymbol{R}_t = \sqrt{2D_R}\boldsymbol{W}_t$, where D_R is the diffusion coefficient and $\boldsymbol{W}_t$ is the standard 2D Brownian motion (BM) or Wiener process [44,49]. An interesting first observation is that the pursuer's stochastic path consists of long runs interrupted by short-time random reorientations (see Fig. 1d). Such a process, known as run-and-tumble motion, has been first observed in bacterium swimming [50]. Our preliminary simulations indicate that this phenomenon emerges naturally in our model for a broad range of parameters. More systematic analysis of the distributions of velocity, tumble angles, running lengths etc., needs to be done to directly link the motion illustrated in Fig. 1d with the run-and-tumble dynamics observed in experiments. This study will be presented in a future paper.

2.2. Stochastic pursuit-evasion model

In this work, we extend the pursuit equation to allow for the prey to evade the predator. Specifically, the modified *stochastic* pursuit-evasion model describes the motion of a predator that stochastically drifts *directly towards* the prey, which in turn, stochastically drifts *directly away* from the predator. Let the drift and diffusivity of the predator be denoted by v_r and D_r, respectively. Similarly, we use v_R and D_R to represent the drift and diffusivity of the prey. The time evolution of the system in d dimensions, where $d = 1, 2,$ and 3, is given by the following system of stochastic differential equations:

$$d\boldsymbol{r}_t = v_r \hat{\boldsymbol{n}}_t dt + \sqrt{2D_r} d\boldsymbol{W}_t^r, \tag{3}$$

$$d\boldsymbol{R}_t = v_R \hat{\boldsymbol{n}}_t dt + \sqrt{2D_R} d\boldsymbol{W}_t^R, \tag{4}$$

where $\hat{\boldsymbol{n}}_t = (\boldsymbol{R}_t - \boldsymbol{r}_t)/\left\|\boldsymbol{R}_t - \boldsymbol{r}_t\right\|$ represents the orientation vector, and $\boldsymbol{W}_t^r$ and $\boldsymbol{W}_t^R$ are d-dimensional independent Wiener processes. The initial positions of the predator and prey are assumed to be $\boldsymbol{r}_0 = 0$ and $\boldsymbol{R}_0 = \boldsymbol{\alpha}_0$, respectively. The difference $\boldsymbol{x}_t = \boldsymbol{R}_t - \boldsymbol{r}_t$ is given by

$$d\boldsymbol{x}_t = -v\hat{\boldsymbol{n}}_t dt + \sqrt{2D} d\boldsymbol{W}_t, \text{ with } \boldsymbol{x}_0 = \boldsymbol{\alpha}_0, \tag{5}$$

where $v = (v_r - v_R)$, $D = D_r + D_R$ and $\boldsymbol{W}_t$ is also a d-dimensional independent Wiener process. This simplified equation provides information about the properties of the distribution of $\boldsymbol{x}_t$, e.g., whether there is a stationary distribution. A more general stochastic pursuit-evasion equation model with anisotropic drift vectors and diffusivity matrices, as well as different types of predator–prey interaction can also be formulated. Here, we have to mention that the interaction term, $(\hat{\boldsymbol{n}}_t)$, is nonlinear. Consequently, the components of the position vectors are not independent as in several OU-based correlated RWs models. Furthermore, for the purpose of this work, the drift of the predator v_r must not be zero, otherwise Eq. (3) would simply describe a Brownian motion. The $\boldsymbol{v}_R$ can be either positive or zero. The case of $\boldsymbol{v}_R = 0$ describes an unsuspected prey performing BM, while for $v_R > 0$ the prey actively evades the predator. Without loss of generality, we assume $D_R = 1$ for the remainder of this paper.

A critical point that we clarify here is the hypothetical underpinnings of the predator–prey dynamics in scenarios where a prey can remain undetectable. In the absence of detectable prey, two critical assumptions are made: first, the predator assumes the existence of prey and takes a "first guess" at the position of this prey $(\boldsymbol{\alpha}_0)$. Second, the predator's guess as to the location of its prey evolves according to the drift–diffusion process of Eq. (4). Parameters of the system, such as the drift velocities and diffusivities may generally be determined by different physiological processes, such as training, natural selection, or both. Similarly, the predator's guess as to the location of prey may also stem from these processes. Therefore, we assume that the predator actively seeks prey regardless of the existence/presence of detectable prey. The existence of the predator's guess makes the predator's motion to be active, which has shown to be an important aspect of foraging, especially in some cases of sparsely distributed fixed targets (e.g., [31]). The absence of the predator's guess would imply the predator has purely passive motion (Brownian motion), contrary to evidence observed in foraging.

There is rich literature on mathematical modeling of pursuit-evasion games (see, for instance, [43,51] and references therein). The stochastic version of such models is usually described by discrete stochastic processes on a two-dimensional lattice. Krapivsky and Redner, for instance, modeled both predators and preys as independent discrete simple RWs [52]. Since both RWs are independent, there is no active pursuit-evasion game. However, a prey is eliminated once it is located on the same site as a predator. Oshanin et al. introduced a short-range interaction between the prey and the predator [53]. Specifically, once a predator and a prey are located in adjacent sites, the predator jumps to the prey's site with probability one, while the prey tries to avoid the predator with probability of < 1 (lazy prey reaction). In both works, the major objective is the detailed analysis of the survival rate. There are a few technical differences between our model and works such as [52,53]. First, our model is a continuous-time stochastic process while those studied in [52,53] are discrete-time models. Second, the interaction range in our case is infinite, while the interaction range for [52,53] is minimal, i.e., it is limited to the same or nearest neighboring site. Third, the objective of each study significantly differs. Refs. [52,53] focus on the survival rate, while our work focuses on the statistical properties of the resulting dynamics. As we will see in the next section, the resulting stochastic process has characteristics observed in various experiments. We hypothesize that such a phenomenological pursuit-evasion game between a predator and a hypothetical prey could possibly model some characteristics of foraging search patterns. We will address in future studies whether the resulting stochastic process is a good candidate for modeling foraging dynamics with direct comparison with existing experimental data.

3. Results and discussion

3.1. One-dimensional case

3.1.1. Persistent random walk with tempered power-law distributed running times

The distribution of running times (or lengths) has perhaps been the single most studied property of stochastic search patterns. Our proposed model describes a generalized persistent random walk with power-law or tempered power-law distributed running times. Such power law distribution is consistent with a large number of experimental observations (see, for example [28,54,55]). It is emphasized that relating experimental data to power-law distributions requires very careful statistical analysis [33,56].

Let us first present the one-dimensional case, where some analytical results are readily derived. Here, the difference equation reduces to:

$$dx_t = -v\,\mathrm{sgn}\,(x_t)\,dt + \sqrt{2D}dW_t, \tag{6}$$

where $\mathrm{sgn}\,(\cdot)$ is the standard sign function. The analysis of Eq. (6) can be divided into three different cases with varying values of relative drift: *(i)* $v > 0$, *(ii)* $v = 0$, and *(iii)* $v < 0$. Each of these scenarios is illustrated as follows.

Case $\boldsymbol{v > 0}$. In this case, where the predator drifts faster than the prey, Eq. (6) simply describes a Brownian motion with dry friction, first postulated by de Gennes in [57]. For large time, the asymptotic solution of Eq. (6) is a stationary Laplace distribution:

$$p_s(x) = \exp(-|x|/x_c)/2x_c, \tag{7}$$

where $x_c = D/v$ [57,58]. This implies that as $t \to \infty$ the average distance between the predator and the prey is always bounded.

Another important characteristic of this case is the probability distribution function (pdf) of the time τ between two consecutive predator–prey encounters. This is a problem of finding the first return time of x_t. In Appendix A, we show that this pdf is a tempered power law distribution with $\mu = 3/2$ and $\tau_c = 4D/v^2$, i.e.,

$$f\,(\tau) \sim \tau^{-3/2} e^{-\tau/(v^2/4D)}. \tag{8}$$

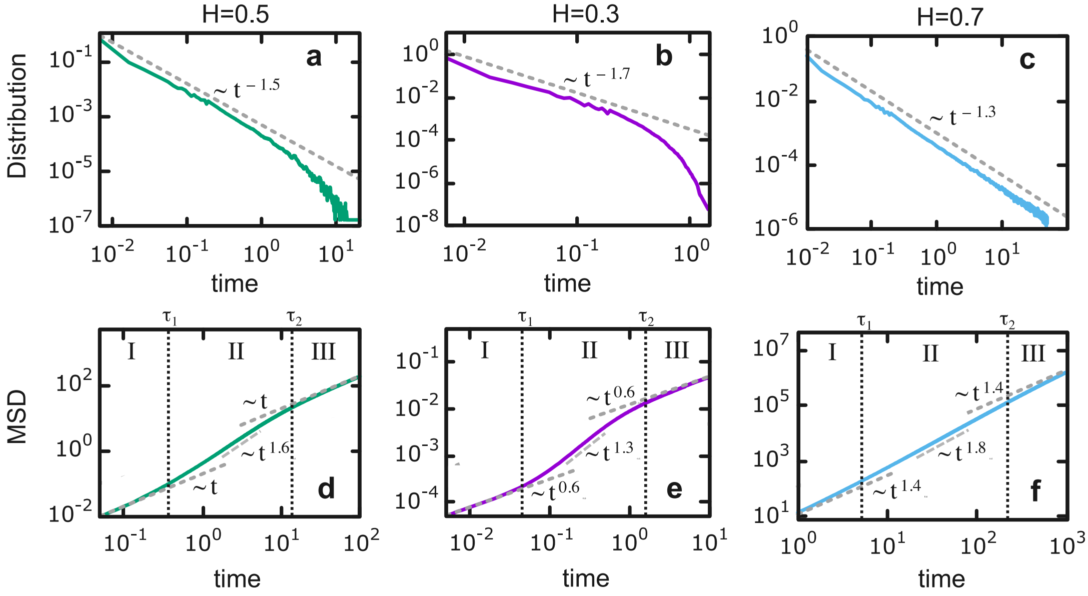

Fig. 2. Statistics of the 1D case. Distribution of running times (top row) and mean squared displacement (MSD) (bottom row) as a function of time for three different values of the Hurst exponent: $H = 0.5$ (first column), $H = 0.3$ (second column), and $H = 0.7$ (third column). In subfigures (d), (e), and (f) the MSD profile is divided into three regions by two critical times τ_1 and τ_2. Specifically, as we move from region I → II → III, we have: (d) diffusive → superdiffusive → diffusive, (e) sub diffusive → superdiffusive → subdiffusive, and (c) superdiffusive → superdiffusive → superdiffusive. The fractional noise is normalized to meet the condition: $\langle W_{H,t}^2 \rangle = 2D_\alpha t^{2H}$, where $\alpha = r$ (predator) or R (prey). In all subfigures, straight lines correspond to numerical results, and the parameters are: ($D_R = 1$, $v_R = 0$, $D_r = 0.1$, $v_r = 1$).

Case $v = 0$. If the drifts of the predator and prey are equal, Eq. (6) describes a Brownian motion (i.e., $x_t = \sqrt{2D}W_t$). This result has two major consequences. First, the average distance between the predator and prey is no longer bounded and, second, the distribution of running times is a pure power-law with $\mu = 3/2$:

$$f(\tau) \sim \tau^{-3/2}. \tag{9}$$

Thus, the predator performs a persistent random walk with power law distributed running times. Due to the divergence of the average and variance of Eq. (9), the process has no characteristic time. This exponent, also known as Sparre-Andersen scaling [59,60], has been discussed before in foraging dynamics [61,62].

Case $v < 0$. If the prey drifts faster than the predator, Eq. (6) can be rewritten as: $dx_t = |v|\text{sgn}(x_t)dt + \sqrt{2D}dW_t$. In this limit, there is finite probability that x_t never returns to zero, and as a consequence the pdf of the running times is defective and cannot be defined [63]. This means that after a finite number of encounters $N \geq 0$, the prey permanently evades the predator. Once x_t reaches the point of no return at time t_N, Eq. (6) becomes a pure drifted Brownian motion (dBM), i.e., $x_{t_N+s} = x_{t_N} \pm |v|\, s + \sqrt{2D}W_s$, where $s \geq 0$.

An interesting observation is that if $v \gg 0$, Eq. (8) approximates an exponential and as a result the corresponding dynamics mimics a Brownian motion. Thus, the stochastic pursuit-evasion model exhibits a transition from Brownian-like motion for $v \gg 0$ to Levy-like walk for $v = 0$ to dBM for $v \ll 0$.

The particular exponent $\mu = 3/2$ that emerges for $v \geq 0$, is a consequence of the BM in Eq. (6). However, if one considers fractional Brownian motion (fBM) instead, then the range of μ broadens. This scenario can be modeled by simply replacing the Brownian motion W_t in Eq. (6) with fractional Brownian motion W_t^H, where $0 < H < 1$ is the Hurst exponent [64]. The fBM is correlated for $H > 1/2$, anticorrelated for $H < 1/2$, while for $H = 1/2$, we have the standard Brownian motion. Following the work of Ref. [65], one can show that for large t the distribution of the running times is

$$f(\tau) \sim \tau^{-(2-H)}. \tag{10}$$

This scaling breaks down when the drift and diffusion spread become comparable. Here, $\mu = 2 - H$, which means that $1 < \mu < 2$. It is noteworthy that random walks with this range of exponents have been extensively discussed in animals foraging literature [24,61,62,66–68].

In Fig. 2a–c, we show the distribution of a predator chasing a Brownian particle for three different values of the Hurst exponent. The parameters of the simulations are: $D_R = 1$, $D_r = 0.1$, $v_R = 0$, and $v_r = 1$. We can clearly see that the results of our numerical simulations are in good agreement with Eq. (10) up to a critical time τ_c. An important outcome of this analysis shows that as $v \to 0^+$ the critical time $\tau_c \to \infty$ leading to pure power-law distributions. In practical situations with finite but long time horizon, such as simulations, experiments or even the real foraging process, the predicted tempered power-law distributions are practically indistinguishable from the corresponding pure power-law distributions [69].

The motion of the predator between two encounter times t_n and t_{n+1} is a dBM towards the positive or negative direction, i.e., $\Delta r_s = \pm v_r s + \sqrt{2D_r}\Delta W_s^r$, where $\Delta r_s = r_{t_n+s} - r_{t_n}$, $\Delta W_s^r = W_{t_n+s}^r - W_{t_n}^r$, $0 < s \leq \tau_n$, and $\tau_n = t_{n+1} - t_n$. In other words, the predator performs a generalized persistent random walk with three important characteristics. First, the running times between two directional changes are tempered power-law distributed. Second, during each running time the predator executes a dBM. Third, the predator's stochastic path is modulated by the prey's movement.

This model can be understood better by directly comparing it with OU-based persistent RW very often used in modeling foraging dynamics. The position of the predator in OU-based models is given by $dr_t^{OU} = v_{OU}(t)\,dt$, where the noise (velocity) $v_{OU}(t)$ is exponentially correlated [4]. In our case, $dr_t = v(t)\,dt + \sigma dW_t^H$, where $v(t) = v_r \mathrm{sgn}(R_t - r_t)$. By noticing that the return times of the difference $R_t - r_t$ follows a tempered power law distribution (see, Eqs. (8) and (9)), the drift $v(t)$ can be viewed as telegraphic noise with tempered power-law distributed waiting times. Additionally, this telegraphic noise is modulated by R_t. Thus, the persistency in our model originates from a telegraphic noise, which is an intrinsic property of the stochastic pursuit-evasion equations. Notably, this simplified view of our model is valid only in 1D. In higher dimensions, the drift term is no longer considered as a telegraphic noise (see Eq. (3)). Similar 1D models of telegraphic processes embedded in BM have recently been reported [70,71]. Specifically, Malakar et al. used Poissonian telegraphic noise [70], while Um et al. implemented Poissonian, Gaussian, and power-law telegraphic noise [71]. There are four main differences between our work and the two previous studies [70,71]. First, our model considers both white and fractional noise, while the above cited works use only white noise. Second, the telegraphic noise in our model is modulated by another stochastic process. Third, the studies in [70,71] have been limited in one-dimension, while our model is straightforwardly applicable in all three dimensions. Fourth, Refs. [70,71] have used Poissonian and power law distributions; in our case power-law distributions are tempered. Interestingly, the limits $v \gg 0$ and $v \to 0^+$ of our model, approximate Poissonian and power-law telegraphic processes, respectively. In summary, our work generalizes [70,71] to (a) consider a modulated tempered-power-law-distributed telegraphic processes coupled with fractional noise, and (b) conveniently extend it in all three dimensions.

3.1.2. Transient superdiffusion

Another characteristic of foraging is the way predators diffuse in space. Consistent with experimental observations [72–75], the pursuit-evasion model predicts superdiffusive or transient superdiffusive motion. The standard way to characterize the diffusive behavior of a stochastic processes r_t is the mean square displacement (MSD) defined as $\left\langle [r_t - r_0]^2 \right\rangle$, where r_0 is the initial condition and $\langle \cdots \rangle$ represents the ensemble average. For fBM, MSD grows as a power of time, i.e., $\left\langle W_{H,t}^2 \right\rangle \sim t^{2H}$. Specifically, for (a) $H = 1/2$ (standard BM), MSD grows linearly in time (diffusion), (b) $H < 1/2$, the process spreads slower than a BM (subdiffusion), and (c) $H > 1/2$, the process spreads faster than a BM (superdiffusion).

Let us first examine the case of $H = 1/2$ (sampling procedure is described in Appendix B). Fig. 2d shows the MSD of a predator chasing a Brownian particle with $D_R > D_r$. Here, we can clearly see the existence of three distinct regions: region I ($t < \tau_1$), region II ($\tau_1 < t < \tau_2$) and region III ($t > \tau_2$). Regions I and II represent the drift–diffusive motion of the predator before catching up with the prey. Here, the MSD is a mixture of diffusive and ballistic motion, i.e., $MSD = 2D_r t + v_r t^2$. For very short times (region I: $t < \tau_1$) the ballistic part of the MSD is negligible, and the diffusion is well approximated by $MSD = 2D_r t$. In the second region, however, the ballistic part of the MSD becomes significant, and the motion turn out to be superdiffusive. For long enough times ($t > \tau_2$), the predator appears to mimic the diffusive trajectory of the prey. In this limit, the MSD becomes linear again, but with enhanced diffusivity $D_R > D_r$, i.e., $MSD = 2D_R t$. In short, as we move from region I → II → III, we have diffusive → superdiffusive → diffusive behavior. This type of transient anomalous diffusion has been observed experimentally [73–75].

Transient superdiffusion is also evident for $H \neq 1/2$. Fig. 2e shows that for $H < 1/2$ there is a subdiffusive → superdiffusive → subdiffusive transition. It is interesting to point out that although regions I and III are subdiffusive, region II is superdiffusive. To the best of our knowledge, such behavior has not been observed experimentally. On the other hand, for $H > 1/2$ (see Fig. 2f), we observe a superdiffusive → superdiffusive → superdiffusive behavior. Note that region II is slightly more superdiffusive than regions I and III. Such anomalous dynamics has been reported in cell migration [72].

Depending on the values of the system parameters, our model can describe other types of transient superdiffusion as well. For instance, for $D_r = 0$ and for $H = 1/2$, the system undergoes a ballistic → diffusive transition. For $v \leq 0$ and $H = 1/2$, as a different example, the predator transitions from an initial diffusive behavior to asymptotic ballistic motion [11,71]. As shown in Section 3.2, all these different types of transient anomalous behavior are also observed in 2D and 3D.

Transient superdiffusion has successfully been modeled using a variety of different stochastic processes [4]. Refs. [70,71] have used a Langevin-type of equation coupled to telegraphic noise, [76–79] are based on $2D$ anisotropic OU models, [80,81] have implemented 2D continuous time RWs, while [72] solves the fractional Klein–Kramers equation. The majority of these works have reported only the diffusive → superdiffusive → diffusive anomalous behavior and only [72] has shown theoretically the existence of superdiffusive → superdiffusive → superdiffusive transition. The authors of [4,80,81] have also reported a ballistic → superdiffusive → diffusive transition. Refs. [70–72,80,81] have been studied in 1D and 2D, respectively, while [76–79] are applicable only in 2D. A practical difference between our work and

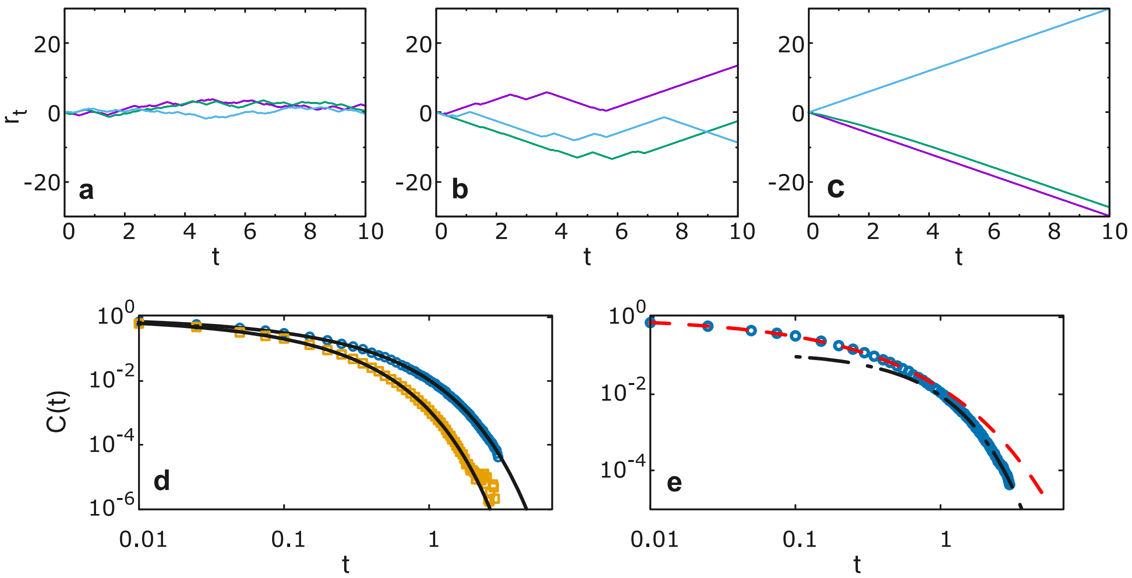

Fig. 3. Directional persistence in 1D. (a), (b), and (c) show three different representative 1D stochastic paths for $v = 2$, $v = 0$, and $v = -2$, respectively ($D_r = 0$, $D_R = 1$). (d) displays log–log plots of the autocorrelation function of the orientation vector versus time. Squares correspond to numerical results for $v = 4$ and circles for $v = 3$. Solid lines represent the analytical result (see Eq. (11)). (e) shows $C(t)$ for $v = 3$ and the corresponding fits of Eqs. (12) (dashed lines) and (13) (dashed–dotted lines). In all subfigures $D_r = 0.1$ and $D_R = 1$.

the aforementioned models is that the stochastic pursuit-evasion equations can reproduce most of these different types of anomalous diffusion in all three dimensions without additional adjustments and modifications.

Although our model captures qualitatively the diffusive behavior observed in a variety of experiments, statistical analysis of other observables, such as persistence and position distributions, is needed to link the stochastic pursuit-evasion curves to the anomalous dynamics of some predators.

3.1.3. Directional persistence

A third interesting experimental observation is that the random reorientations of predators are correlated [15,72,82–86]. Here, we show that our approach predicts strongly correlated stochastic paths, with correlation times that diverge near $v \approx 0$. Below, we analyze the directional persistence of our model in 1D and for $H = 1/2$. Similar behavior is observed in 2D and 3D systems (see next subsection).

A first qualitative understanding of the directional persistence is obtained by simply observing representative stochastic paths for different values of the drift v. Fig. 3a–c show that the paths appear to be random for positive drift (Fig. 3a), intermediately persistent for $v = 0$ (Fig. 3b), and increasingly very persistent for negative drift (Fig. 3c). Thus, we observe that our model exhibits a transition from low persistency to high persistency as the drift crosses zero from positive values.

A more rigorous way of studying the persistency of a stochastic process is through autocorrelation functions. In most experimental and theoretical works, the persistence of foraging paths is usually detected through the velocity autocorrelation function. In our model, since the Wiener process is nowhere differentiable [87], the instantaneous velocity of the predator cannot be defined (see Eq. (3). A very recent theoretical analysis argues that similar issues may exist even in experimental measurements [88]. To avoid this mathematical limitation, we studied the persistency in our model through the autocorrelation of the orientational vector $\hat{\boldsymbol{n}}_t$, $C(t) = \langle \hat{\boldsymbol{n}}_0 \cdot \hat{\boldsymbol{n}}_t \rangle$.

In 1D and for $v > 0$, the orientational vector has a known stationary solution [57,58]. In Appendix C, we show that the autocorrelation function of $\hat{n}_t = \mathrm{sgn}(x_t)$ is given by

$$C\,(t) = \left(2\frac{t}{\tau_c} + 1\right) \mathrm{erfc}\left(\sqrt{\frac{t}{\tau_c}}\right) - \sqrt{\frac{4}{\pi}\frac{t}{\tau_c}} \exp\left(-\frac{t}{\tau_c}\right), \tag{11}$$

where $\mathrm{erfc}\,(\cdot)$ is the complementary error function and $\tau_c = 4D/v^2$ is defined as the correlation time. Consequently, the correlation time diverges as $v \to 0$.

Fig. 3d shows the time evolution of $C(\tau)$ for two different values of the drift. We can clearly see that the autocorrelation function relaxes faster with increasing v. We also observe an excellent match of the numerical prediction with Eq. (11). Furthermore, we observe that, for short times, $C(\tau)$ is characterized by a slow relaxation, which eventually become pure exponential. Interestingly, the slow relaxation of $C(\tau)$ can be well fitted by a stretched exponential. Thus, Eq. (11) can be approximated by

$$C\,(t) \approx \mathrm{e}^{-(t/t_c)^b}, \text{ for } t < t_* \tag{12}$$

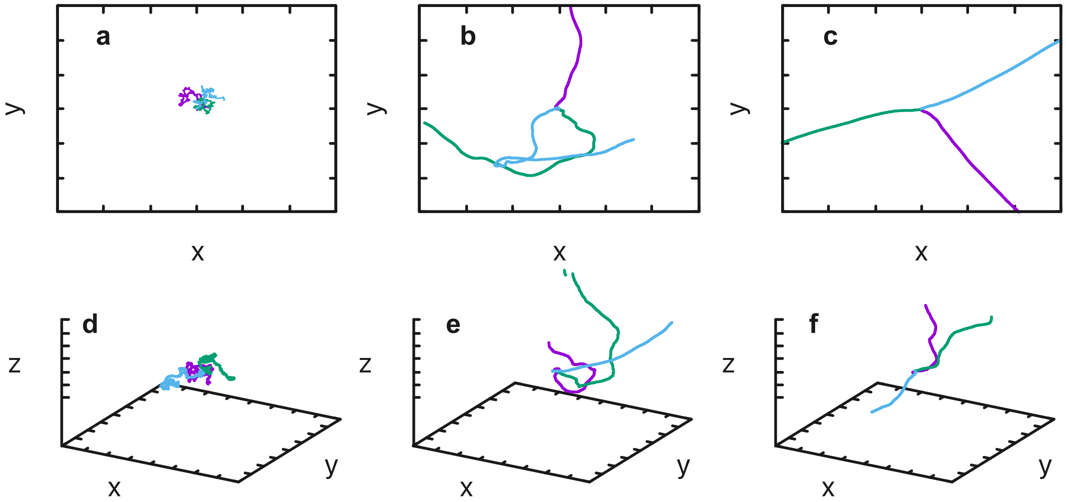

Fig. 4. Three representative stochastic paths in 2D (top row) and 3D (bottom row) for $v = 2$ (first column), $v = 0$ (second column), and $v = -2$ (third column). In all subfigures $D_r = 0.1$, $D_R = 1$, and $H = 1/2$.

and

$$C(t) \approx e^{-t/T_c}, \text{ for } t > t_* \tag{13}$$

where t_* is the switch time between stretched and pure exponential, t_c and T_c denote the corresponding correlation times, and $0 < b \leq 1$ is the stretching exponent. In Fig. 3e, we see that $t_* \approx 1$ and the stretched exponential is an adequate approximation for up to two orders of magnitude drop of the autocorrelation function.

3.2. Two- and three-dimensional cases

In this section, we briefly present numerical results of the 2D and 3D stochastic pursuit-evasion model for $H = 1/2$.

In Fig. 4a–c and d–f representative trajectories of the 2D and 3D model, respectively, for different values of the relative drift v are shown. Similar to 1D case, the stochastic paths are very random for $v \gg 0$, intermediately persistent for $v \approx 0$, and highly persistent for $v \ll 0$.

Fig. 5 shows the main statistical properties of the 2D and 3D stochastic pursuit-evasion curves. Specifically, in Fig. 5a, we show that the running times follow a tempered power-law distribution with exponent $\mu = 3/2$. Similar to the 1D case if one considers fractional noise, i.e., $H \neq 1/2$ then $1 < m < 2$. The transient superdiffusive behavior of the predator is presented in Fig. 5b. As we can clearly see, the diffusive → superdiffusive → diffusive transition is maintained in both 2D and 3D curves. In general, by adjusting the parameters of the system accordingly, all the different types of transient anomalous dynamics discussed in Section 3.1.2 are preserved in 2D and 3D. Figs. 5c and 5d exhibit the orientational autocorrelation function in 2D and 3D, respectively. The dashed and dashed–dotted lines represent the best fit of a stretched exponential (Eq. (12)) and a pure exponential (Eq. (13)). We see that Eq. (12) fits very well the numerical simulation for up to one to two orders of magnitude drop of the $C(\tau)$. Similar to 1D the autocorrelation function relaxes slower with decreasing v and ultimately diverges for $v \to 0^+$.

Overall, this section demonstrates that the major characteristics of the 1D pursuit-evasion model are maintained in 2D and 3D without additional modifications.

4. Summary

A central assumption of this work was that foraging dynamics emerge from the strong coupling between predators and prey. Predators move randomly to locate prey who simultaneously move randomly to avoid predators. To develop such a stochastic process, we built upon the traditional pursuit model. Specifically, we assumed that predators drift stochastically towards prey and prey respond by drifting away from predators. This coupled process can be modeled by what we call stochastic pursuit-evasion curves described by Eqs. (3) and (4). If the position of the prey is known, this model can approximate features of chemotaxis. In the absence of any external stimuli, predators assume the existence of prey and actively continue their foraging pattern.

From the purely mathematical point of view, the stochastic pursuit-evasion curves are described by a persistent random walk with three key properties: (a) the predator executes drifted Brownian motion between two consecutive directional changes, (b) the corresponding running times are drawn from tempered power-law distributions, and (c) the predator's

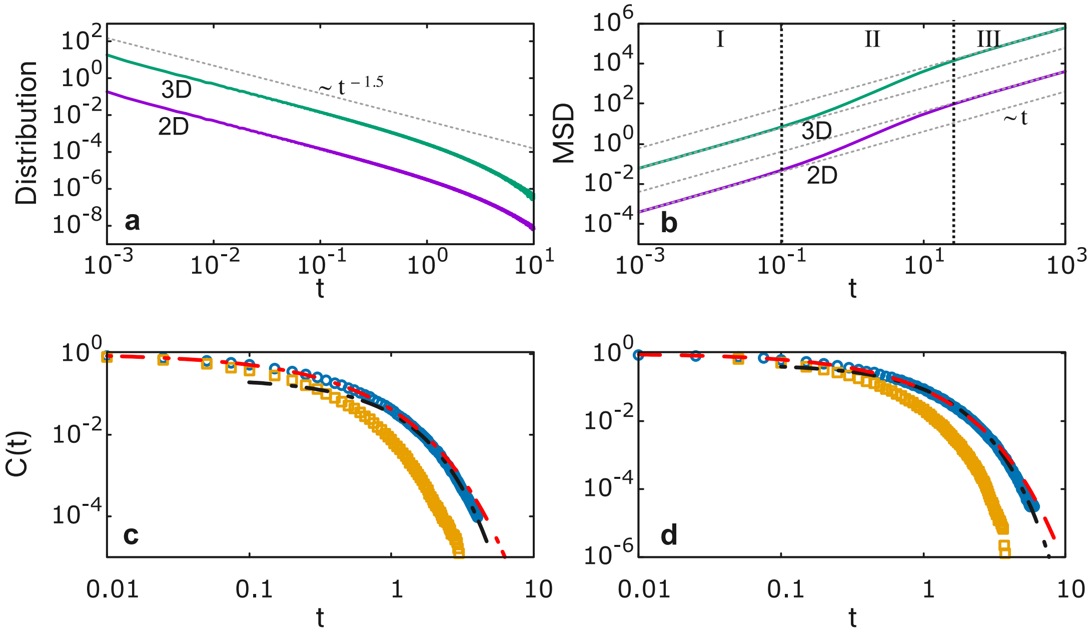

Fig. 5. Model statistics in 2D and 3D. Top row shows the log–log plot of the 2D and 3D (a) distribution of running times and (b) MSD as a function of time. The curves for the 3D cases have been shifted upwards for clarity. In both subfigures $\upsilon = 1$. Bottom row displays the log–log plots of the autocorrelation function of the orientation vector versus time in (c) 2D and (d) 3D. Squares correspond to numerical results for $\upsilon = 4$ and circles for $\upsilon = 3$. Dashed line and dashed–dotted line in (e) represent fits of Eqs. (12) and (13), respectively. In all subfigures: $D_r = 0.1$, $D_R = 1$, and $H = 1/2$.

dynamics are instantly modulated by the prey's position. Such a stochastic process has several interesting properties. First, there is a transition from dBM for $\upsilon \ll 0$ to LW-like patterns for $\upsilon = 0$ and BM-like behavior for $\upsilon \gg 0$. Second, predators exhibit rich anomalous or transient anomalous dynamics. Third, the directional vector of predators shows a strong correlation with correlation times that diverge as $\upsilon \to 0$. Such properties have been observed and discussed in a variety of experimental and theoretical works.

Although we have demonstrated a qualitative agreement with some experimental measurements, more systematic work is required to link our model with specific foraging patterns. Such analysis certainly requires a direct comparison of the stochastic pursuit-evasion curves with experimental data. This question will be thoroughly investigated in a future work. Furthermore, in future studies, we plan to explore cases of (a) different types of noise (e.g., colored noise), (b) alternative prey dynamics, such as LWs, intermittent RWs, or other continuous-time RWs, and (c) more complex pursuit-evasion strategies [51,89].

CRediT authorship contribution statement

Kellan Toman: Conceptualization, Methodology, Investigation, Formal analysis, Software, Writing – original draft, Writing – review & editing. **Nikolaos K. Voulgarakis:** Conceptualization, Supervision, Methodology, Investigation, Formal analysis, Software, Writing – original draft, Writing – review & editing.

Declaration of competing interest

The authors declare that they have no known competing financial interests or personal relationships that could have appeared to influence the work reported in this paper.

Acknowledgments

We thank the two anonymous reviewers for their careful reading of the manuscript and their insightful suggestions. NKV acknowledges support from the National Science Foundation, United States of America (Grant No. 1951583).

Appendix A. Distribution of predator–prey encounter times

Here, we show the validity of Eqs. (8) and (9). Let the initial condition for the difference be $x_0 = a_0$, and, without loss of generality, assume that $a_0 > 0$. The difference x_t is positive until the first predator–prey encounter, and consequently

x_t executes a simple dBM i.e., $x_t = -vt + \sqrt{2D}W_t$. Let t_1 be the time immediately after the first encounter and denote $x_{t_1} = a_1 < 0$. The same process is repeated with a new initial condition a_1 till x_t changes sign again. Finding the probability distribution function of $\tau_j = t_{j+1} - t_j$, where $j = 1, 2, \ldots$, is equivalent to the first passage time problem of a drift–diffusion process over a level a_j. The solution to this problem for any $a > 0$, presented by Smoluchowski and Schrödinger in 1915 [90,91], is given by the inverse Gaussian or Wald distribution:

$$f\left(\tau; a\right) = \frac{a}{2\sqrt{\pi D}}\tau^{-3/2}\exp\left[-\frac{(a - v\tau)^2}{4D\tau}\right]. \tag{A.1}$$

An important remark is that a can be as small as possible, but not zero. If $a = 0$, x_t may cross the origin infinite times and as a result the probability distribution cannot be defined [65]. Eq. (A.1) can be rewritten as:

$$f\left(\tau\right) = \frac{a}{\sqrt{4\pi D}}\exp\left(\frac{av}{2D}\right)\exp\left(-\frac{a^2}{4D\tau}\right)\tau^{-3/2}\exp\left(-\frac{\tau}{4D/v^2}\right). \tag{A.2}$$

The first two factors in the above equation are constants for given a, while the third factor is only significant for short times of the order or smaller than $\alpha^2/4D$. Note that $|a| \leq |dx_t|$, and thus, a is in general very small. For intermediate times only the fourth and fifth factor contribute to the distribution, i.e.,

$$f\left(\tau\right) \sim \tau^{-3/2}\exp\left(-\frac{\tau}{4D/v^2}\right). \tag{A.3}$$

This is simply Eq. (8); a tempered power law distribution with $\mu = 3/2$ and $\tau_c = 4D/v^2$ (see Eq. (1)). Note that the scaling does not depend on a.

If $v = 0$, then Eq. (A.1) converges to the Lévy (or Lévy–Smirnov) distribution:

$$f\left(\tau; \overline{\alpha}\right) = \frac{a}{2\sqrt{\pi D}}\tau^{-3/2}\exp\left[-\frac{a^2}{4D\tau}\right]. \tag{A.4}$$

This equation reduces to Eq. (9) for $\tau \gg a^2/4D$.

Appendix B. Sampling

We have tested that for $v > 0$, the difference $\boldsymbol{x}_t$ always reaches a stationary solution. To ensure that statistical averages are sampled from this state, we implement the following equilibration procedure. The initial conditions of the predator and prey are always $r_0 = 0$ and $R_0 \sim p_s\left(R_0\right)$, respectively (see Eq. (7)). The initial condition for $x_0 = R_0 - r_0$ is very close to the stationary solution. We then integrate Eqs. (3) and (4) up to a time t_{eq} to ensure that the system has reached its stationary state. Statistical sampling always starts after t_{eq}. We have tested numerically that this equilibration procedure ensures that ensemble and time averages match. It may be noted that for $H = 1/2$ and $d = 1$, Eq. (7) is already the exact stationary distribution and extra equilibration is not required. For $v \leq 0$, the system does not have a stationary solution, and thus, this equilibration procedure is not applicable. Here, we have to mention that the pursuit-evasion game is still valid even if the system starts far away from equilibrium.

Appendix C. Orientational autocorrelation function

The propagator for the one-dimensional Brownian motion with dry friction is given by:

$$p\left(\tilde{x}, \tilde{t}|\tilde{x}', 0\right) = \frac{e^{-\tilde{t}/4}}{2\sqrt{\pi\tilde{t}}}e^{-(|\tilde{x}|-|\tilde{x}'|)/2}e^{-(\tilde{x}-\tilde{x}')^2/(4\tilde{t})} + \frac{e^{-|\tilde{x}|}}{4}\left[1 + \operatorname{erf}\left(\frac{\tilde{t} - (|\tilde{x}| - |\tilde{x}'|)}{2\sqrt{\tilde{t}}}\right)\right],$$

where $\tilde{t} = (v^2/D)t$ and $\tilde{x} = (v/D)x$ [58]. Thus, the autocorrelation function of the orientational vector $n_t = \operatorname{sgn}\left(x_t\right)$ is:

$$\left\langle\hat{n}_0\hat{n}_t\right\rangle = \int_{-\infty}^{\infty}\int_{-\infty}^{\infty}\operatorname{sgn}\left(\tilde{x}\right)\operatorname{sgn}\left(\tilde{x}'\right)p\left(\tilde{x}, t|\tilde{x}', 0\right)p_s\left(\tilde{x}'\right)d\tilde{x}'d\tilde{x},$$

where $p_s(x)$ is the stationary distribution given by Eq. (7). Straightforward integration gives Eq. (11).

References

[1] G.H. Pyke, Optimal foraging theory: A critical review, Annu. Rev. Ecol. Syst. 15 (1984) 523–575, http://dx.doi.org/10.1146/annurev.es.15.110184.002515.

[2] E.M. Fèvre, B.M.D.C. Bronsvoort, K.A. Hamilton, S. Cleaveland, Animal movements and the spread of infectious diseases, Trends Microbiol. 14 (2006) 125–131, http://dx.doi.org/10.1016/j.tim.2006.01.004.

[3] K.M. Yamada, M. Sixt, Mechanisms of 3D cell migration, Nat. Rev. Mol. Cell Biol. 20 (2019) 738–752, http://dx.doi.org/10.1038/s41580-019-0172-9.

[4] V. Méndez, D. Campos, F. Bartumeus, Stochastic Foundations in Movement Ecology, Springer Berlin Heidelberg, Berlin, 2014, http://dx.doi.org/10.1007/978-3-642-39010-4.

[5] G.M. Viswanathan, M.G.E. da Luz, E.P. Raposo, H.E. Stanley, The Physics of Foraging: An Introduction To Random Searches and Biological Encounters, Cambridge University Press, 2011, http://dx.doi.org/10.1017/CBO9780511902680.

[6] D. Boyer, G. Ramos-Fernández, O. Miramontes, J.L. Mateos, G. Cocho, H. Larralde, H. Ramos, F. Rojas, Scale-free foraging by primates emerges from their interaction with a complex environment, Proc. R. Soc. B Biol. Sci. 273 (2006) 1743–1750, http://dx.doi.org/10.1098/rspb.2005.3462.

[7] D. Boyer, O. Miramontes, H. Larralde, Lévy-like behaviour in deterministic models of intelligent agents exploring heterogeneous environments, J. Phys. A Math. Theor. 42 (2009) 434015, http://dx.doi.org/10.1088/1751-8113/42/43/434015.

[8] M.S. Abe, Functional advantages of Lévy walks emerging near a critical point, Proc. Natl. Acad. Sci. USA 117 (2020) 24336–24344, http://dx.doi.org/10.1073/pnas.2001548117.

[9] A.M. Reynolds, F. Bartumeus, A. Kolzsch, J. Van De Koppel, Signatures of chaos in animal search patterns, Sci. Rep. 6 (2016) 23492, http://dx.doi.org/10.1038/srep23492.

[10] S.C. Nicolis, J. Fernández, C. Pérez-Penichet, C. Noda, F. Tejera, O. Ramos, D.J.T. Sumpter, E. Altshuler, Foraging at the edge of chaos: Internal clock versus external forcing, Phys. Rev. Lett. 110 (2013) 268104, http://dx.doi.org/10.1103/PhysRevLett.110.268104.

[11] V. Zaburdaev, S. Denisov, J. Klafter, Lévy walks, Rev. Modern Phys. 87 (2015) 483–530, http://dx.doi.org/10.1103/RevModPhys.87.483.

[12] M.F. Shlesinger, J. Klafter, Lévy walks versus Lévy flights, in: Growth Form, Springer, Netherlands, 1986, pp. 279–283, http://dx.doi.org/10.1007/978-94-009-5165-5_29.

[13] G.E. Uhlenbeck, L.S. Ornstein, On the theory of the Brownian motion, Phys. Rev. 36 (1930) 823, http://dx.doi.org/10.1103/PhysRev.36.823.

[14] G.A. Dunn, A.F. Brown, A unified approach to analysing cell motility, J. Cell Sci. (1987) 81–102, http://dx.doi.org/10.1242/jcs.1987.Supplement_8.5.

[15] D. Selmeczi, S. Mosler, P.H. Hagedorn, N.B. Larsen, H. Flyvbjerg, Cell motility as persistent random motion: Theories from experiments, Biophys. J. 89 (2005) 912–931, http://dx.doi.org/10.1529/biophysj.105.061150.

[16] A.M. Reynolds, L. Leprêtre, D.A. Bohan, Movement patterns of tenebrio beetles demonstrate empirically that correlated-random-walks have similitude with a Lévy walk, Sci. Rep. 3 (2013) 1–8, http://dx.doi.org/10.1038/srep03158.

[17] A.M. Reynolds, Can spontaneous cell movements be modelled as Lévy walks? Phys. A Stat. Mech. Appl. 389 (2010) 273–277, http://dx.doi.org/10.1016/j.physa.2009.09.027.

[18] T.S. Biró, A. Jakovác, Power-law tails from multiplicative noise, Phys. Rev. Lett. 94 (2005) 132302, http://dx.doi.org/10.1103/PhysRevLett.94.132302.

[19] M. Auger-Méthé, A.E. Derocher, M.J. Plank, E.A. Codling, M.A. Lewis, Differentiating the Lévy walk from a composite correlated random walk, Methods Ecol. Evol. 6 (2015) 1179–1189, http://dx.doi.org/10.1111/2041-210X.12412.

[20] O. Bénichou, M. Coppey, M. Moreau, P.-H. Suet, R. Voituriez, Optimal search strategies for hidden targets, Phys. Rev. Lett. 94 (2005) 198101, http://dx.doi.org/10.1103/PhysRevLett.94.198101.

[21] M.A. Lomholt, K. Tal, R. Metzler, K. Joseph, Lévy strategies in intermittent search processes are advantageous, Proc. Natl. Acad. Sci. 105 (2008) 11055–11059, http://dx.doi.org/10.1073/PNAS.0803117105.

[22] O. Bénichou, C. Loverdo, M. Moreau, R. Voituriez, Intermittent search strategies, Rev. Modern Phys. 83 (2011) 81, http://dx.doi.org/10.1103/RevModPhys.83.81.

[23] G. Ariel, A. Be'Er, A. Reynolds, Chaotic model for Lévy walks in swarming bacteria, Phys. Rev. Lett. 118 (2017) 228102, http://dx.doi.org/10.1103/PhysRevLett.118.228102.

[24] G.M. Viswanathan, S.V. Buldyrev, S. Havlin, M.G.E. Da Luz, E.P. Raposo, H.E. Stanley, Optimizing the success of random searches, Nature 401 (1999) 911–914, http://dx.doi.org/10.1038/44831.

[25] D.W. Sims, E.J. Southall, N.E. Humphries, G.C. Hays, C.J.A. Bradshaw, J.W. Pitchford, A. James, M.Z. Ahmed, A.S. Brierley, M.A. Hindell, D. Morritt, M.K. Musyl, D. Righton, E.L.C. Shepard, V.J. Wearmouth, R.P. Wilson, M.J. Witt, J.D. Metcalfe, Scaling laws of marine predator search behaviour, Nature 451 (2008) 1098–1102, http://dx.doi.org/10.1038/nature06518.

[26] T.H. Harris, E.J. Banigan, D.A. Christian, C. Konradt, E.D.T. Wojno, K. Norose, E.H. Wilson, B. John, W. Weninger, A.D. Luster, A.J. Liu, C.A. Hunter, Generalized Lévy walks and the role of chemokines in migration of effector CD8 + T cells, Nature 486 (2012) 545–548, http://dx.doi.org/10.1038/nature11098.

[27] G.C. Hays, T. Bastian, T.K. Doyle, S. Fossette, A.C. Gleiss, M.B. Gravenor, V.J. Hobson, N.E. Humphries, M.K.S. Lilley, N.G. Pade, D.W. Sims, High activity and Lévy searches: Jellyfish can search the water column like fish, Proc. R. Soc. B Biol. Sci. 279 (2012) 465–473, http://dx.doi.org/10.1098/rspb.2011.0978.

[28] N.E. Humphries, N. Queiroz, J.R.M. Dyer, N.G. Pade, M.K. Musyl, K.M. Schaefer, D.W. Fuller, J.M. Brunnschweiler, T.K. Doyle, J.D.R. Houghton, G.C. Hays, C.S. Jones, L.R. Noble, V.J. Wearmouth, E.J. Southall, D.W. Sims, Environmental context explains levy and Brownian movement patterns of marine predators, Nature (2010) http://dx.doi.org/10.1038/nature09116.

[29] D.W. Sims, A.M. Reynolds, N.E. Humphries, E.J. Southall, V.J. Wearmouth, B. Metcalfe, R.J. Twitchett, Hierarchical random walks in trace fossils and the origin of optimal search behavior, Proc. Natl. Acad. Sci. USA 111 (2014) 11073–11078, http://dx.doi.org/10.1073/pnas.1405966111.

[30] A.M. Reynolds, A.D. Smith, R. Menzel, U. Greggers, D.R. Reynolds, J.R. Riley, Displaced honey bees perform optimal scale-free search flights, Ecology 88 (2007) 1955–1961, http://dx.doi.org/10.1890/06-1916.1.

[31] D.A. Raichien, B.M. Wood, A.D. Gordon, A.Z.P. Mabuiia, F.W. Marlowe, H. Pontzer, Evidence of Lévy walk foraging patterns inhuman hunter-gatherers, Proc. Natl. Acad. Sci. USA 111 (2014) 728–733, http://dx.doi.org/10.1073/pnas.1318616111.

[32] D.W. Sims, N.E. Humphries, N. Hu, V. Medan, J. Berni, Optimal searching behaviour generated intrinsically by the central pattern generator for locomotion, Elife 8 (2019) http://dx.doi.org/10.7554/eLife.50316.

[33] A. Reynolds, Liberating Lévy walk research from the shackles of optimal foraging, Phys. Life Rev. 14 (2015) 59–83, http://dx.doi.org/10.1016/j.plrev.2015.03.002.

[34] A.M. Edwards, R.A. Phillips, N.W. Watkins, M.P. Freeman, E.J. Murphy, V. Afanasyev, S.V. Buldyrev, M.G.E. Da Luz, E.P. Raposo, H.E. Stanley, G.M. Viswanathan, Revisiting Lévy flight search patterns of wandering albatrosses, bumblebees and deer, Nature 449 (2007) 1044–1048, http://dx.doi.org/10.1038/nature06199.

[35] A.M. Edwards, Overturning conclusions of Lévy flight movement patterns by fishing boats and foraging animals, Ecology 92 (2011) 1247–1257, http://dx.doi.org/10.1890/10-1182.1.

[36] G.H. Pyke, Understanding movements of organisms: it's time to abandon the Lévy foraging hypothesis, Methods Ecol. Evol. 6 (2015) 1–16, http://dx.doi.org/10.1111/2041-210X.12298.

[37] V.V. Palyulin, A.V. Chechkin, R. Metzler, Lévy flights do not always optimize random blind search for sparse targets, Proc. Natl. Acad. Sci. 111 (2014) 2931–2936, http://dx.doi.org/10.1073/PNAS.1320424111.

[38] N. Levernier, J. Textor, O. Bénichou, R. Voituriez, Inverse square Lévy walks are not optimal search strategies for d≥2, Phys. Rev. Lett. 124 (2020) 080601, http://dx.doi.org/10.1103/PhysRevLett.124.080601.

[39] S.V. Buldyrev, E.P. Raposo, F. Bartumeus, S. Havlin, F.R. Rusch, M.G.E. Da Luz, G.M. Viswanathan, Comment on inverse square Lévy walks are not optimal search strategies for d≥2, Phys. Rev. Lett. 126 (2021) http://dx.doi.org/10.1103/PHYSREVLETT.126.048901.

[40] N. Levernier, J. Textor, O. Bénichou, R. Voituriez, Reply to comment on 'Inverse square Lévy walks are not optimal search strategies for d≥2 ', Phys. Rev. Lett. 126 (2021) http://dx.doi.org/10.1103/PHYSREVLETT.126.048902.

[41] B. Guinard, A. Korman, Intermittent inverse-square Lévy walks are optimal for finding targets of all sizes, Sci. Adv. 7 (2021) http://dx.doi.org/10.1126/SCIADV.ABE8211.

[42] T. Dannemann, D. Boyer, O. Miramontes, Lévy flight movements prevent extinctions and maximize population abundances in fragile Lotka–Volterra systems, Proc. Natl. Acad. Sci. USA 115 (2018) 3794–3799, http://dx.doi.org/10.1073/pnas.1719889115.

[43] P.J. Nahin, Chases and Escapes : The Mathematics of Pursuit and Evasion, 2012, p. 253.

[44] G. Cabrera, Pursuit problems: Generalizations and numerical simulations, 2011.

[45] P. Bouguer, Lignes de poursuite, in: Mémoires L'Académie R. Des Sci, L'Imprimerie Royale, Paris, 1732, pp. 1–14.

[46] G. Boole, A Treatise on Differential Equations, Macmillan and Co, London, 1877.

[47] P.E. Kloeden, E. Platen, in: Peter E. Kloeden, Eckhard Platen (Eds.), Numerical Solution of Stochastic Differential Equations, Springer-Verlag Berlin, New York, 1992.

[48] https://works.bepress.com/gmcnamara/18/, No Title, (n.d.). https://works.bepress.com/gmcnamara/18/.

[49] R. Anderson, Uncertainty-Anticipating Stochastic Optimal Feedback Control of Autonomous Vehicle Models, University of California, Santa Cruz, 2014, https://escholarship.org/uc/item/3400q1w1 (Accessed 24 November 2020).

[50] H.C. Berg, D.A. Brown, Chemotaxis in escherichia coli analysed by three-dimensional tracking, Nature 239 (1972) 500–504, http://dx.doi.org/10.1038/239500a0.

[51] G. Miller, D. Cliff, Co-Evolution of Pursuit and Evasion I: Biological and Game-Theoretic Foundations, University of Sussex, Brighton, UK, 1994, http://www.opengrey.eu/item/display/10068/594624 (Accessed 27 October 2021).

[52] P.L. Krapivsky, S. Redner, Kinetics of a diffusive capture process: lamb besieged by a pride of lions, J. Phys. A. Math. Gen. 29 (1996) 5347, http://dx.doi.org/10.1088/0305-4470/29/17/011.

[53] G. Oshanin, O. Vasilyev, P.L. Krapivsky, J. Klafter, Survival of an evasive prey, Proc. Natl. Acad. Sci. 106 (2009) 13696–13701, http://dx.doi.org/10.1073/PNAS.0904354106.

[54] S. Huda, B. Weigelin, K. Wolf, K.V. Tretiakov, K. Polev, G. Wilk, M. Iwasa, F.S. Emami, J.W. Narojczyk, M. Banaszak, S. Soh, D. Pilans, A. Vahid, M. Makurath, P. Friedl, G.G. Borisy, K. Kandere-Grzybowska, B.A. Grzybowski, Lévy-like movement patterns of metastatic cancer cells revealed in microfabricated systems and implicated in vivo, Nature Commun. 9 (2018) 1–11, http://dx.doi.org/10.1038/s41467-018-06563-w.

[55] H. Murakami, T. Niizato, T. Tomaru, Y. Nishiyama, Y.P. Gunji, Inherent noise appears as a Lévy walk in fish schools, Sci. Rep. 5 (2015) 10605, http://dx.doi.org/10.1038/srep10605.

[56] M.E. Wosniack, M.C. Santos, E.P. Raposo, G.M. Viswanathan, M.G.E. da Luz, The evolutionary origins of Lévy walk foraging, PLoS Comput. Biol. 13 (2017) e1005774, http://dx.doi.org/10.1371/journal.pcbi.1005774.

[57] P.G. De Gennes, Brownian motion with dry friction, J. Stat. Phys. 119 (2005) 953–962, http://dx.doi.org/10.1007/s10955-005-4650-4.

[58] H. Touchette, E. Van der Straeten, W. Just, Brownian motion with dry friction: Fokker–Planck approach, J. Phys. A Math. Theor. 43 (2010) 445002, http://dx.doi.org/10.1088/1751-8113/43/44/445002.

[59] E.S. Andersen, On the fluctuations of sums of random variables, Math. Scand. 1 (1953) 263–285, http://dx.doi.org/10.7146/math.scand.a-10385.

[60] E.S. Andersen, On the fluctuations of sums of random variables II, Math. Scand. 2, 195–223.

[61] A.M. Reynolds, Scale-free movement patterns arising from olfactory-driven foraging, Phys. Rev. E. 72 (2005) 041928, http://dx.doi.org/10.1103/PhysRevE.72.041928.

[62] A. Reynolds, E. Ceccon, C. Baldauf, T.K. Medeiros, O. Miramontes, Lévy foraging patterns of rural humans, PLoS One. 13 (2018) e0199099, http://dx.doi.org/10.1371/JOURNAL.PONE.0199099.

[63] S. Karlin, H.E. Taylor, A First Course in Stochastic Processes, Elsevier, Science, 2012.

[64] B.B. Mandelbrot, J.W. Van Ness, Fractional brownian motions, fractional noises and applications, SIAM Rev. 10 (1968) 422–437, http://dx.doi.org/10.1137/1010093.

[65] M. Ding, W. Yang, Distribution of the first return time in fractional Brownian motion and its application to the study of on-off intermittency, Phys. Rev. E. 52 (1995) 207–213, http://dx.doi.org/10.1103/PhysRevE.52.207.

[66] G.M. Viswanathan, V. Afanasyev, S.V. Buldyrev, E.J. Murphy, P.A. Prince, H.E. Stanley, Lévy flight search patterns of wandering albatrosses, Nature 381 (1996) 413–415, http://dx.doi.org/10.1038/381413a0.

[67] E.P. Raposo, F. Bartumeus, M.G.E. da Luz, P.J. Ribeiro-Neto, T.A. Souza, G.M. Viswanathan, How landscape heterogeneity frames optimal diffusivity in searching processes, PLoS Comput. Biol. 7 (2011) e1002233, http://dx.doi.org/10.1371/journal.pcbi.1002233.

[68] E.P. Raposo, S.V. Buldyrev, M.G.E. da Luz, M.C. Santos, H.E. Stanley, G.M. Viswanathan, Dynamical robustness of Lévy search strategies, Phys. Rev. Lett. 91 (2003) 240601, http://dx.doi.org/10.1103/PhysRevLett.91.240601.

[69] R.N. Mantegna, H.E. Stanley, Stochastic process with ultraslow convergence to a Gaussian: The truncated Lévy flight, Phys. Rev. Lett. (1994).

[70] K. Malakar, V. Jemseena, A. Kundu, K.V. Kumar, S. Sabhapandit, S.N. Majumdar, S. Redner, A. Dhar, Steady state, relaxation and first-passage properties of a run-and-tumble particle in one-dimension, J. Stat. Mech. Theory Exp. 2018 (2018) 043215, http://dx.doi.org/10.1088/1742-5468/AAB84F.

[71] J. Um, T. Song, J.-H. Jeon, Langevin dynamics driven by a telegraphic active noise, Front. Phys. (2019) 143, http://dx.doi.org/10.3389/FPHY.2019.00143.

[72] P. Dieterich, R. Klages, R. Preuss, A. Schwab, Anomalous dynamics of cell migration, Proc. Natl. Acad. Sci. USA 105 (2008) 459–463, http://dx.doi.org/10.1073/pnas.0707603105.

[73] C. Metzner, C. Mark, J. Steinwachs, L. Lautscham, F. Stadler, B. Fabry, Superstatistical analysis and modelling of heterogeneous random walks, Nature Commun. 6 (2015) 1–8, http://dx.doi.org/10.1038/ncomms8516.

[74] H. Rajakaruna, J. O'Connor, I.A. Cockburn, V.V. Ganusov, Liver environment-imposed constraints diversify movement strategies of liver-localized CD8 T cells, 2021, http://dx.doi.org/10.1101/2020.11.06.371690, BioRxiv.

[75] P.H. Wu, A. Giri, S.X. Sun, D. Wirtz, Three-dimensional cell migration does not follow a random walk, Proc. Natl. Acad. Sci. USA 111 (2014) 3949–3954, http://dx.doi.org/10.1073/pnas.1318967111.

[76] B. ten Hagen, S. van Teeffelen, H. Löwen, Brownian motion of a self-propelled particle, J. Phys. Condens. Matter. 23 (2011) 194119, http://dx.doi.org/10.1088/0953-8984/23/19/194119.

[77] F. Peruani, L.G. Morelli, Self-propelled particles with fluctuating speed and direction of motion in two dimensions, Phys. Rev. Lett. 99 (2007) 010602, http://dx.doi.org/10.1103/PhysRevLett.99.010602.

[78] I. Fortuna, G.C. Perrone, M.S. Krug, E. Susin, J.M. Belmonte, G.L. Thomas, J.A. Glazier, R.M.C. de Almeida, CompuCell3D simulations reproduce mesenchymal cell migration on flat substrates, Biophys. J. 118 (2020) 2801–2815, http://dx.doi.org/10.1016/j.bpj.2020.04.024.

[79] C. Kurzthaler, S. Leitmann, T. Franosch, Intermediate scattering function of an anisotropic active Brownian particle, Sci. Rep. 61 (6) (2016) 1–11, http://dx.doi.org/10.1038/srep36702, 2016.

[80] D. Campos, V. Ḿndez, Superdiffusive-like motion of colloidal nanorods, J. Chem. Phys. 130 (2009) 134711, http://dx.doi.org/10.1063/1.3102096.

[81] G.M. Viswanathan, E.P. Raposo, F. Bartumeus, J. Catalan, M.G.E. Da Luz, Necessary criterion for distinguishing true superdiffusion from correlated random walk processes, Phys. Rev. E - Stat. Nonlinear Soft Matter Phys. 72 (2005) 011111, http://dx.doi.org/10.1103/PHYSREVE.72.011111/FIGURES/2/MEDIUM.

[82] S. Vedel, S. Tay, D.M. Johnston, H. Bruus, S.R. Quake, Migration of cells in a social context, Proc. Natl. Acad. Sci. USA 110 (2013) 129–134, http://dx.doi.org/10.1073/pnas.1204291110.
[83] T.D. Yang, J.-S. Park, Y. Choi, W. Choi, T.-W. Ko, Zigzag turning preference of freely crawling cells, PLoS One 6 (2011) 20255, http://dx.doi.org/10.1371/journal.pone.0020255.
[84] L. Li, S.F. Nørrelkke, E.C. Cox, Persistent cell motion in the absence of external signals: A search strategy for eukaryotic cells, PLoS One 3 (2008) http://dx.doi.org/10.1371/journal.pone.0002093.
[85] R. Gorelik, A. Gautreau, Quantitative and unbiased analysis of directional persistence in cell migration, Nat. Protoc. 9 (2014) 1931–1943, http://dx.doi.org/10.1038/nprot.2014.131.
[86] E.R. Jerison, S.R. Quake, Heterogeneous T cell motility behaviors emerge from a coupling between speed and turning in vivo, Elife 9 (2020) 1–26, http://dx.doi.org/10.7554/eLife.53933.
[87] I. Karatzas, S.E. Shreve, Brownian Motion and Stochastic Calculus, Springer, New York, 1991.
[88] G.L. Thomas, I. Fortuna, G.C. Perrone, J.A. Glazier, J.M. Belmonte, R.M.C. de Almeida, Phys. A Stat. Mech. Appl. 550 (2020) 124493, http://dx.doi.org/10.1016/j.physa.2020.124493.
[89] D. Weihs, P.W. Webb, Optimal avoidance and evasion tactics in predator–prey interactions, J. Theoret. Biol. 106 (1984) 189–206, http://dx.doi.org/10.1016/0022-5193(84)90019-5.
[90] M. von Smoluchowski, Notiz¨uber die berechnung der brownschen molekularbewegung bei der Ehrenhaft-Millikan'schen versuchsanordnung, Phys. Z. XVI (1915) 318–321.
[91] E. Schrodinger, Zur theorie der fall- und steigversuche an teilchen mit brownscher bewegung, Phys. Z. 16 (1915) 289–295.